Journal of Alzheimer's Disease 48 (2015) 995–1008
DOI 10.3233/JAD-150311
IOS Press

Novel Cortical Thickness Pattern for Accurate Detection of Alzheimer's Disease

Weihao Zheng, Zhijun Yao, Bin Hu*, Xiang Gao, Hanshu Cai, Philip Moore and for the Alzheimer's Disease Neuroimaging Initiative[1]
School of Information Science and Engineering, Lanzhou University, Lanzhou, China

Handling Associate Editor: Zhanjun Zhang

Accepted 14 July 2015

Abstract. Brain network occupies an important position in representing abnormalities in Alzheimer's disease (AD) and mild cognitive impairment (MCI). Currently, most studies only focused on morphological features of regions of interest without exploring the interregional alterations. In order to investigate the potential discriminative power of a morphological network in AD diagnosis and to provide supportive evidence on the feasibility of an individual structural network study, we propose a novel approach of extracting the correlative features from magnetic resonance imaging, which consists of a two-step approach for constructing an individual thickness network with low computational complexity. Firstly, multi-distance combination is utilized for accurate evaluation of between-region dissimilarity; and then the dissimilarity is transformed to connectivity via calculation of correlation function. An evaluation of the proposed approach has been conducted with 189 normal controls, 198 MCI subjects, and 163 AD patients using machine learning techniques. Results show that the observed correlative feature suggests significant promotion in classification performance compared with cortical thickness, with accuracy of 89.88% and area of 0.9588 under receiver operating characteristic curve. We further improved the performance by integrating both thickness and apolipoprotein E $\varepsilon 4$ allele information with correlative features. New achieved accuracies are 92.11% and 79.37% in separating AD from normal controls and AD converters from non-converters, respectively. Differences between using diverse distance measurements and various correlation transformation functions are also discussed to explore an optimal way for network establishment.

Keywords: Alzheimer's disease, combined distance, correlation calculation function, cortical thickness network, magnetic resonance imaging, mild cognitive impairment

INTRODUCTION

Alzheimer's disease (AD) is a progressive, irreversible, and currently incurable neurodegenerative disease and the most common form of dementia. Previous studies have suggested that the early onset of dementia is characterized by cognitive decline, short-term memory loss, language decrease, and increasing aggression [1–5]. In fact, AD is a major social and geopolitical problem impacting societies and governments globally [6–8] as evidenced by the prevalence of the condition. Brookmeyer et al. have observed that, in 2007, AD affected 26.6 million people globally and the prediction is that by 2050, around 1 in 85 people will develop this condition [9]. It has been noted that dementia accounts for between 50% to 80% of AD cases, and mild cognitive impairment (MCI) is widely considered to be the transitional stage between normal aging and dementia [10, 11]. MCI is characterized by memory impairment while general cognitive and

[1]Data used in preparation of this article were obtained from the Alzheimer's Disease Neuroimaging Initiative (ADNI) database (http://adni.loni.usc.edu). As such, the investigators within the ADNI contributed to the design and implementation of ADNI and/or provided data but did not participate in analysis or writing of this report. A complete listing of ADNI investigators can be found at: http://adni.loni.usc.edu/wp-content/uploads/how_to_apply/ADNI_Acknowledgement_List.pdf

*Correspondence to: Bin Hu, No. 222 Tianshui Road, Lanzhou, Gansu 730000, China. Tel.: +86 18993168389; E-mail: bh@lzu.edu.cn.

ISSN 1387-2877/15/$35.00

functional abilities are usually retained. A comparison between patients suffering from MCI and normal controls (NC) demonstrates that for healthy individuals a conversion to full AD occurs at a rate of 1% to 2% per year, whereas the conversion rate for patients with MCI occurs at an annualized rate of 10% to 15% [12–14].

Research into the human brain can be traced back over many decades [15–19]. Since subjects with MCI tend to progress to AD with relatively high proportion per year, it is urgent to effectively classify MCI, especially progressive MCI (pMCI), and AD for early diagnosis and efficient treatment, which may hopefully delay the conversion, along with preventing pMCI progression and AD deterioration. With the rapid development of brain imaging techniques and gene-analytic techniques, many valuable biomarkers which can effectively identify AD and MCI have been identified in the literature. Apolipoprotein E (APOE) $\varepsilon 4$ allele is reported as a major genetic risk factor increasing 10 to 12-fold risk for late-onset AD compare to $\varepsilon 3$ homozygotes [20, 21]. Furthermore, such genotype has become part and parcel of biomarker discovery and accuracy promotion in classification works [22–25]. Recent studies have also focused on investigating the characteristics in brain network connections [26–29], with the majority of published research supporting the conclusion that cognitive and memory decline in patients with AD is tied to the changes in brain networks [26, 29–33]. With in-depth studies, connectivity-based classification approaches were gradually developed, especially in functional magnetic resonance imaging (fMRI) and diffusion tensor imaging (DTI), obtaining more than 90% accuracy [34–38]. As MRI is the most standardized, easily available imaging modality, several recent studies focused on constructing an individual morphological network. For example, Raj et al. constructed a single-subject correlation matrix with regional cortical thickness, volume, and curvature to distinguish temporal lobe epilepsy from healthy individuals [39]. Wee et al. and Dai et al. have expressed similar views [40, 41], which calculate the thickness network via exponential function.

These studies of individual structural network construction fail to take into account vertex-based information, which we suppose may arguably represent more detailed information [42, 43]. Also, we hypothesize that the selection of correlation calculation function could significantly affect the connectivity strength. In the present study, we propose a cortical thickness based two-step network construction approach, including dissimilarity estimation and connectivity transformation. Firstly, the combined distance (the combination of region-to-region distance and vertex-to-region distance) is defined as the dissimilarity measurement between pairs of regions of interest (ROIs). Secondly, we utilize correlation calculation function to transform dissimilarity into connectivity. The inverse proportional function (INP), which could directly reflect the relationship between dissimilarity and correlation rather than other functions, is introduced and compared with exponential function. Machine learning approaches were applied to evaluate the performance of the proposed network. Results showed that the correlative characteristic could significantly improve the classification performance when compared with cortical thickness. Besides, obvious improvement could be observed when using the combined distance, as well as the novel correlation calculation function. APOE genotype was also utilized to further improve the performance. To our knowledge, there are few acknowledged approaches to MRI-based individual network construction, our method provides proof of effectiveness of morphological network application in AD diagnosis, and further exploration is needed within such domain.

The remainder of the article is structured as follows: The next section describes the methodology in detail, which includes the construction of individual networks, feature selection, and the classification framework; and then the results derived from testing are presented, followed by a discussion which concludes our findings, limitations, and potential future directions.

MATERIALS AND METHODS

Data acquisition

Data used in the preparation of this article were obtained from the Alzheimer's Disease Neuroimaging Initiative (ADNI) database (http://adni.loni.usc.edu). The ADNI was launched in 2003 as a public-private partnership, led by Principal Investigator Michael W. Weiner, MD. The primary goal of ADNI has been to test whether serial MRI, positron emission tomography, other biological markers, and clinical and neuropsychological assessment can be combined to measure the progression of MCI and early AD. For up-to-date information, see http://www.adni-info.org.

The MCI subjects were divided into two categories: patients who would convert to AD in 36 months were considered as progressive MCI (pMCI); and subjects who would not convert to AD in the same period of time were considered to be stable MCI (sMCI).

Table 1
Characteristics of the participants involved in this study

Variables	NC	sMCI	pMCI	AD
No. of subjects (Male / Female)	189 (89 / 100)	94 (52 / 42)	104 (62 / 42)	163 (81 / 82)
Age (mean ± SD)	76.2 ± 5.2	75.4 ± 6.9	74.9 ± 7.3	75.8 ± 7.2
CDR	0	0.5	0.5	0.5 / 1
MMSE (mean ± SD)	29.2 ± 0.9	27.2 ± 1.8	26.7 ± 2.4	23.3 ± 2.1
APOE $\varepsilon 4$ allele population (%)	29.10%	43.62%	63.46%	70.55%

NC, normal controls; sMCI, stable mild cognitive impairment; pMCI, progressive mild cognitive impairment; AD, Alzheimer's disease; CDR, Clinical Dementia Rating; MMSE, Mini-Mental State Examination; APOE, apolipoprotein.

Additionally, the baseline 1.5T structural MRI scans were used as the input data and the baseline clinical cognitive examinations were reevaluated at specified intervals (6 or 12 months). Table 1 illustrates the demographic information of the participants, and the general inclusion criteria are as follows:

- Normal controls (NCs) have received the Mini-Mental State Examination (MMSE) [44] between 24 and 30 (inclusive) and a Clinical Dementia Rating (CDR) [45] of zero. All NCs were non-depressed having no cognitive impairment or mental disorder.
- MCI subjects had MMSE scores between 24 and 30 (inclusive), a CDR of 0.5, with memory complaint, absence of significant levels of impairment in other cognitive domains, while essentially preserved activities of daily living, and an absence of dementia.
- AD patients had MMSE scores between 18 and 26 (inclusive), CDR of 0.5 or 1.

Classification framework

The classification framework shown in Fig. 1 has been divided into three steps:

1) Image pre-processing and feature extraction: all T1-weighted images were pre-processed by FreeSurfer software (http://surfer.nmr.mgh.harvard.edu/). The N3 algorithm [46] was utilized to correct for intensity non-uniformity. After segmentation and the pial surface achievement, we calculated the cortical thickness by computing the mean of the two shortest distances between the white matter and pial surfaces. Then the individual morphological correlation network could be constructed by using the methodology introduced in next subsection.
2) Feature selection: find optimal discriminative features to help identification. In this paper, a two-step feature selection method was applied to reduce the dimension of training feature set and to select a subset with complementary information.
3) Classification: A kernel-based SVM classifier was trained via the selected features.

Construction of the individual network

For dissimilarity measurement, region-to-region distance is commonly utilized as the rough representation of between-region difference [40, 41, 47]; however, such rough distance did not take into consideration the relationships between vertices in different regions, which would probably lose some detailed information. One solution to this problem is to use more precise evaluation. As vertex-to-vertex distance has a huge computational cost, we propose that the precision distance serve as the difference between each vertex cortical thickness and regional mean cortical thickness, combined with rough distance to form a novel estimation of interregional dissimilarity (see Equation 1 and 2).

$$d_{precision}(a,b) = \frac{1}{m}\sum_{i=1}^{m}\left|t_a^i - \overline{t_b}\right|\frac{1}{n}\sum_{j=1}^{n}\left|t_b^j - \overline{t_a}\right| \quad (a \neq b) \tag{1}$$

$$d_{rough}(a,b) = \left|\overline{t_a} - \overline{t_b}\right|^2 \tag{2}$$

where m and n are the number of vertices in region a and region b, respectively, t_a^i denotes the thickness at ith vertex of region a, and $\overline{t_b}$ is the mean cortical thickness of region b. Obviously, we may obtain a nonzero number between the same region (if $a = b$) by using Equation 1. It was incompatible with the definition of the correlation, as the correlation between one region and itself may not equal to 1. Hence, we only calculated the distance between different regions and set those from the same region directly to 0. Then the combined distance, regarded as the dissimilarity between two brain regions, could be defined as follow:

$$d(a,b) = \sqrt{d_{precision}(a,b) + d_{rough}(a,b)} \tag{3}$$

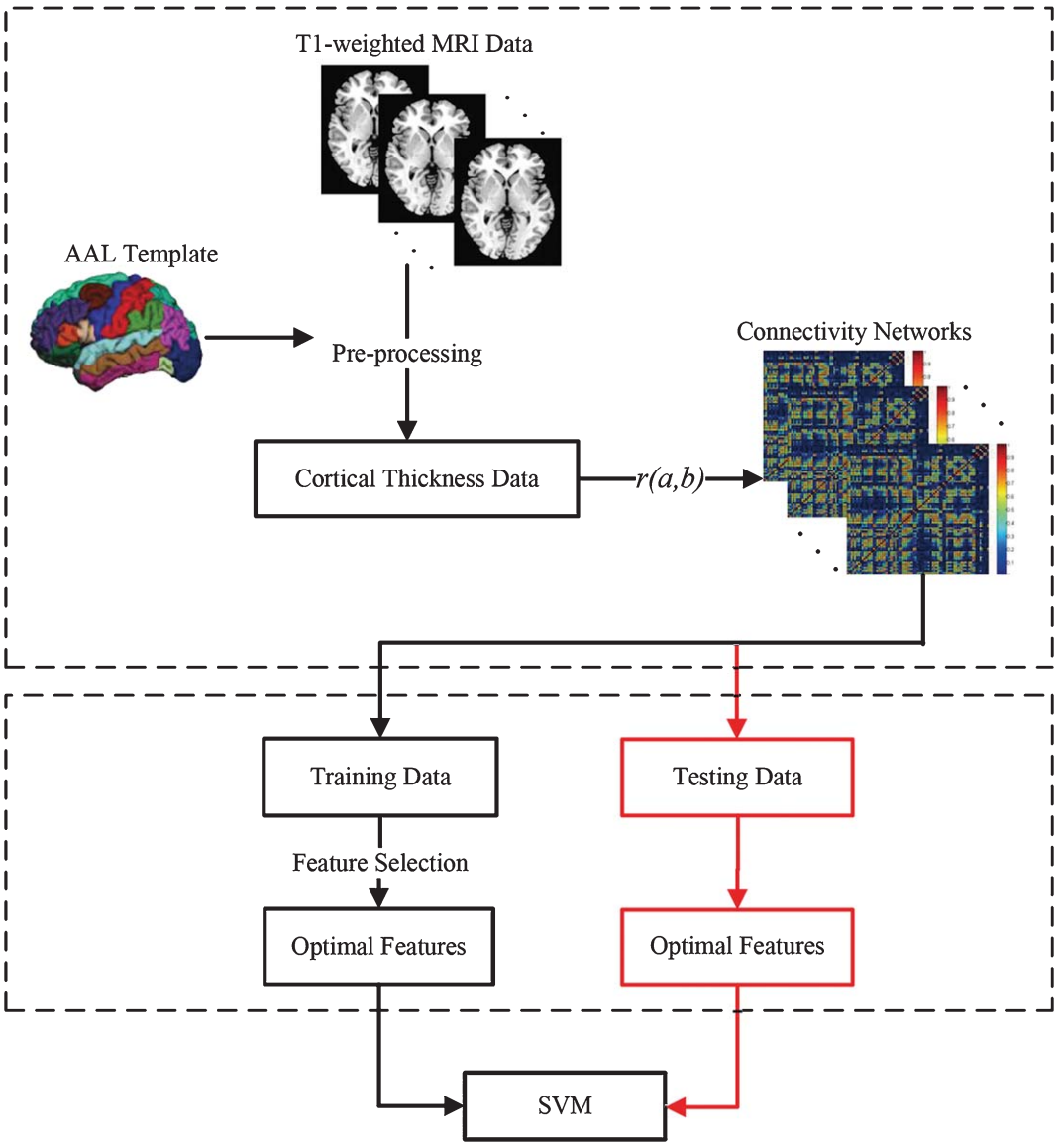

Fig. 1. The proposed classification framework.

It should be worth noting that we removed the subcortical tissues of Automated Anatomical Labeling [48] template, and the remaining 78 cortical regions were utilized to construct a 78×78 correlative matrix. Prior to the correlation calculation, t-test and Chi-square test were implemented to test the differences in age and gender, respectively. No significant differences ($p > 0.05$) were found between each of the two groups in age as well as in gender.

After the dissimilarity calculation, the correlation calculation function based on the inverse-proportional function was proposed, where σ_a and σ_b are the standard deviation of region a and region b, respectively. We chose the INP function because of its nonlinearity, boundness, and direct reflection of the inverse proportional trend to the dissimilarity. Additionally, the standard deviation is used to improve individual diversity and dissimilarity magnitude.

$$r(a, b) = \frac{1}{d/2(\sigma_a + \sigma_b) + 1} \tag{4}$$

Based on the analysis above, a 78×78 diagonal symmetry correlation matrix of each subject was obtained. The average maps of three groups are shown

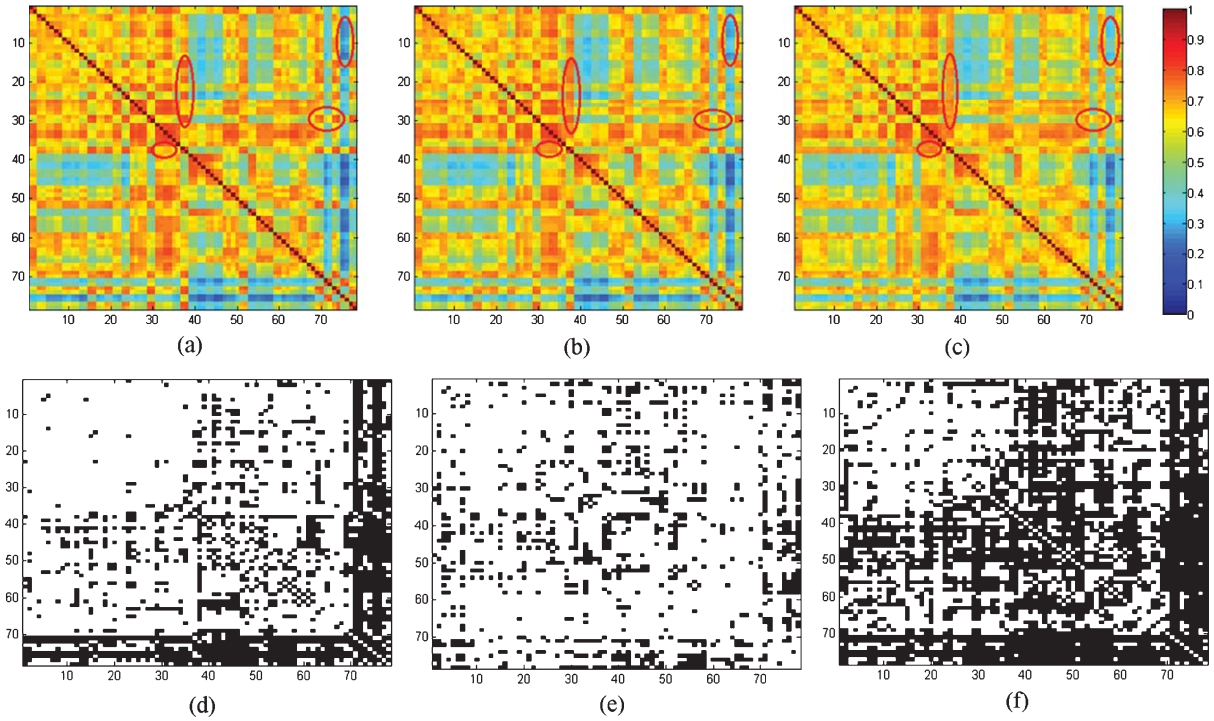

Fig. 2. (a), (b) and (c) are the average network of NC, MCI, and AD group, respectively. They look similar, but a few differences could be found (see the red circle). The second row shows the between-group differences of correlations ($p < 0.05$, BH-FDR corrected): (d) NC versus MCI, (e) MCI versus AD, (f) NC versus AD. The difference between AD and NC is the maximum.

in the first line of Fig. 2. The upper triangle of each matrix was extracted and concatenated to form a feature vector with a length of $78 \times (78 - 1)/2 = 3003$.

Feature selection

The most discriminative and characterizing features are chosen through feature selection to guarantee the low error rate. Besides, feature selection is used for dimensionality reduction, data minimization, redundancy minimization, and calculation reduction [49, 50]. In our study, a two-step feature selection method, including minimum redundancy and maximum relevance (mRMR) [51] and support vector machine recursive feature elimination (SVM-RFE) [52] were utilized.

mRMR is a well-known filter method, providing two balances: 1) between efficiency and broadness, and 2) between relevance and redundancy [40, 51]. The relevance and redundancy are measured by mutual information. While maximizing the mutual information between each feature and label vector, it minimized the redundancy between each feature pair. The Feature Selection Toolbox (FEAST) v1.1.1 [53], which provides implementations of common mutual information based filter feature selection algorithms, was implemented in the mRMR computation process. Before mRMR selection, the feature variables were discretized into three types using the unsupervised method described in [51]. However, mRMR does not consider feature complementarity and the selected feature set may not be optimal. For example, features with low discriminative power may contribute to the final result if they are complementary to others. To deal with that, we removed a small number of features when using mRMR and applied SVM-RFE for further feature selection. SVM-RFE aims to find an optimal feature set that gains the best performance for SVM classifier. To achieve this goal, we applied the linear-based kernel function to calculate the error rate and evaluate the feature performance. Features with small weights are removed during each SVM training interaction.

Classification

Based on the selected features above, the commonly used classifier SVM [54] was chosen for classification. We applied LIBSVM library [55] on MATLAB, and radial basis function (RBF) kernel was utilized because

of its good performance, especially on small sample problems [56]. The RBF kernel is defined as follow:

$$K(x_1, x_2) = \exp\left(-\frac{\|x_1 - x_2\|^2}{2\sigma^2}\right) \quad (5)$$

where x_1 and x_2 are two feature vectors, and σ is the width of the Gaussian kernel. The classification procedure was performed via a 10-fold cross-validation (CV) and repeated 10 times. In each interaction, the subjects were divided into 10 subsets, one of them was selected as testing set, and the reminders were used for feature selection and classifier training. We also applied a grid search optimization algorithm and 3-fold cross-validation to select optimal SVM parameters.

RESULTS

Comparison with cortical thickness data

In this subsection, we made a comparison of classification and prediction performances between cortical thickness and the correlative feature we proposed. Additionally, APOEε4 allele was also considered as an important component, providing outstanding contribution for accuracy improvement [57]. Mean classification accuracy, sensitivity, specificity, and AUC were calculated as the variables for performance estimation.

As is shown in Table 2, the performances of cortical thickness were not satisfactory in all classification tasks, and the classifying ability met a significant improvement when using the correlative features. In particular, we achieved the accuracy of 89.88% in distinguishing AD patients from healthy controls with a high AUC of 0.9588, sensitivity of 80.01%, and specificity of 98.85%. In MCI versus NC and AD versus MCI, the accuracy of 85.43% and 84.89%, respectively, were obtained, both exceeded more than 12% compared to the thickness data. Thus the correlative feature derived from thickness, as the indirect characteristic, surpassed its original form. It is also worth noting that the AUCs of our method in all the tasks were larger than 0.91, indicating high precision of classification. Additionally, the specificity for classifying AD and NC reached 98.85%. Similar results were obtained in combined connectivity with cortical thickness and APOEε4 allele, as significant improvements can only be found in AD versus NC ($p < 0.05$). When integrating all these features, further improvements were observed, particularly we achieved accuracy of 92.11% and AUC of 0.9622 in AD classification.

Table 3 shows that our approach performs much better than those only using cortical thickness in AD conversion prediction, which achieved the accuracy and AUC of 75.19% and 0.8580, respectively, and greatly improved the prediction accuracy by more than 13%. The performance showed a greatly increasing trend when combining these two features, as accuracy of 78.38% and AUC of 0.8611 were obtained. Also, we found that APOEε4 allele information contributed to the prediction promotion, though not as much as cortical thickness; the final accuracy integrating various features significantly increased to 79.37%, with sensitivity of 78.89%, specificity of 79.88%, and AUC of 0.8546. Another point worth noting is cortical thickness could provide complementary information when

Table 3
Prediction performance of different features

Feature	sMCI versus pMCI			
	ACC (%)	SEN (%)	SPE (%)	AUC
Thickness	61.81	83.87	38.48	0.5518
Correlative	75.19	76.61	74.33	0.8580
TH + Correlative	78.38	78.44	78.39	0.8611
APOE + Correlative	75.94	73.03	77.55	0.8084
Combined	79.37	78.89	79.88	0.8546

sMCI, stable mild cognitive impairment; pMCI, progressive mild cognitive impairment; ACC, accuracy; SEN, sensitivity; SPE, specificity; AUC, area under ROC curve; TH, regional mean cortical thickness; APOE, apolipoprotein; Combined, combination of thickness, APOE, and correlative feature.

Table 2
Classification performance of different features

Feature	AD versus NC				AD versus MCI				MCI versus NC			
	ACC (%)	SEN (%)	SPE (%)	AUC	ACC (%)	SEN (%)	SPE (%)	AUC	ACC (%)	SEN (%)	SPE (%)	AUC
Thickness	81.21	71.88	89.68	0.8807	67.40	42.04	86.26	0.5378	73.20	72.80	74.17	0.8047
Correlative	89.88	80.01	98.85	0.9588	84.89	77.52	90.29	0.9133	85.43	85.24	85.62	0.9341
TH + Correlative	90.48	88.91	91.90	0.9607	83.99	80.39	86.76	0.9191	84.81	84.99	85.07	0.9220
APOE + Correlative	90.78	88.75	92.58	0.9574	84.79	79.17	87.92	0.9068	85.61	84.25	87.92	0.8995
Combined	92.11	89.89	94.31	0.9622	85.86	80.59	89.91	0.9203	86.93	87.78	85.83	0.9250

AD, Alzheimer's disease; NC, normal controls; MCI, mild cognitive impairment; TH, regional mean cortical thickness; APOE, apolipoprotein; ACC, accuracy; SEN, sensitivity; SPE, specificity; AUC, area under ROC curve; Combined, combination of thickness, APOE, and correlative feature.

Table 4
Classification performance of different construction functions

Construction method	AD versus NC				AD versus MCI				MCI versus NC			
	ACC (%)	SEN (%)	SPE (%)	AUC	ACC (%)	SEN (%)	SPE (%)	AUC (%)	ACC (%)	SEN (%)	SPE (%)	AUC
Rough + INP	88.46	93.24	82.93	0.9133	82.28	87.24	75.16	0.8919	83.69	83.27	85.23	0.8976
Rough + EXP	88.21	83.15	92.86	0.9194	80.67	72.16	86.93	0.8821	84.29	84.87	83.73	0.9138
Precision + INP	86.61	84.23	86.92	0.8993	76.63	65.94	86.12	0.7921	76.48	79.06	73.57	0.8446
Precision + EXP	84.32	79.68	88.95	0.8685	75.60	77.13	73.44	0.7840	74.59	62.18	82.74	0.7997
Combined + INP	89.88	80.01	98.85	0.9588	84.89	77.52	90.29	0.9133	85.43	85.24	85.62	0.9341

AD, Alzheimer's disease; NC, normal controls; MCI, mild cognitive impairment; ACC, accuracy; SEN, sensitivity; SPE, specificity; AUC, area under ROC curve; INP, inverse proportional function; EXP, exponential function; Combined, Combined distance.

classifying AD-likes (AD and pMCI) from NC-likes (NC and sMCI).

Comparison of distance and correlation calculation function

In this subsection, we made two comparisons including: 1) the performance of using rough distance, precision distance, and combined distance; 2) the performance of the connectivity calculated via different functions, e.g., exponential function (EXP) Wee et al. proposed [40] and inverse proportional function. We suppose that combined distance network would probably preserve some detailed information, and connectivity function selection could also be an influential factor to final result. Comparison results can be observed in both Tables 4 and 5.

Compared with precision distance, rough distance provided more separation information, as its performances outperformed the others in all classification tasks. However, this does not imply that the lower performed distance can be ignored. Since the accuracies we obtained from precision distance was still much higher than random classification (50% accuracy), some effective characteristics should exist. The combined distance, preserving such helpful characteristics, surpassed the rough distance when using the same correlation calculation function. Specifically, combined distance correlations separately achieved the accuracies of 89.88%, 84.89%, and 85.43% in classifying AD, MCI, and NC, which significantly surpassed rough distance correlation ($p < 0.05$).

Results also suggested that INP might be more suitable to reflect the relationship between dissimilarity and connectivity. For example, in all precision distance tasks, INP function yields nominally higher accuracies than EXP function, although differences were not significant in MCI versus AD ($p = 0.057$). Besides, the INP function achieved significantly more accurate performances in distinguishing AD ($p = 0.034$) and MCI ($p = 0.048$) from NC in rough distance tasks. We achieved the best accuracy in separating MCI-AD converters from non-converters, which exceeds 2.73% compared with the rough-EXP connectivity. Also, the rough-INP correlation significantly surpasses the EXP correlation by improving the accuracy to 74.86% ($p = 0.037$). Figure 4 illustrates the ROC curve of these combinations in AD-NC classification and AD conversion prediction; both of them show the connectivity we proposed had the largest AUCs.

Table 5
Prediction performance of different construction functions

Construction method	sMCI versus pMCI			
	ACC (%)	SEN (%)	SPE (%)	AUC
Rough + INP	74.86	70.98	78.79	0.8160
Rough + EXP	72.46	71.91	73.91	0.8052
Precision + INP	72.38	75.58	69.73	0.7824
Precision + EXP	71.29	66.75	75.49	0.7740
Combined + INP	75.19	76.61	74.33	0.8580

sMCI, stable mild cognitive impairment; pMCI, progressive mild cognitive impairment; ACC, accuracy; SEN, sensitivity; SPE, specificity; AUC, area under ROC curve; INP, inverse proportional function; EXP, exponential function; Combined, Combined distance.

Discriminative correlations

We utilized *t*-test with threshold of 0.05 to find the discriminative connections. Benjamini and Hochberg's false discovery rate (BH-FDR) control algorithm, which is to find the maximum i meets $p_i < i * 0.05/n$ ($n = 3003$), was performed to correct the comparison [58, 59]. Before statistical analysis, we performed a linear regression to remove the effect of age. Despite the similarity among the average maps of three groups in the first line of Fig. 2, differences (see the red circle) were observed. In the AD group, the connectivity between parahippocampal gyri and orbital frontal gyri shows a decreasing trend, while the connectivities between parahippocampal gyri and cingulum gyri shows an increasing trend, which is consistent

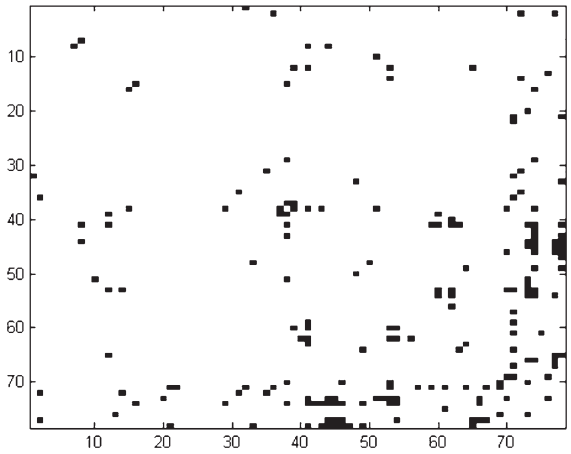

Fig. 3. Difference between sMCI and pMCI ($p < 0.05$, BH-FDR corrected).

with the previous findings [33]. In addition, the connectivities between areas: temporal pole and insula, insula and parahippocampal gyri, parahippocampal gyri and supplementary motor were all observed as decreasing trends in AD patients. The MCI group shows the same variation tendency as AD, indicating MCI is the transitional stage of AD. In the second line of Fig. 2, significant differences exist in the connectivity related to areas: temporal lobe, parahippocampal gyri, precuneus, cuneus, and olfactory cortex in NC versus AD. The edges connecting parahippocampal gyri, temporal pole, lingual gyri, angular gyri, precuneus, and cingulum gyri, which demonstrate significant between-group differences in NC versus MCI. Figure 3 indicates only a 3.33% connectivity difference between sMCI and pMCI, which is much lower than other between-group difference proportions shown in Fig. 2, e.g., AD versus NC (51.02%), MCI versus NC (26.77%), and MCI versus AD (15.85%), corresponding to the fact that the boundary of these two subgroups has not yet been clearly defined.

Top 20 discriminative correlations listed in Table 6 for separating MCI-AD converters from non-converters were selected via *t*-test and BH-FDR correction. It was observed that the discriminative correlations not only appeared in the side of hemisphere, but rather widely existed in the whole brain. The abnormal regions include: bilateral parahippocampal gyri, cingulum gyri, angular gyri, lingual guri, insula, postcenteral gyri, precuneus, insula, supramarginal gyru, occipital lobe, and temporal lobe, all of which are considered to be the regions with significant differences in MCI [60]. Most connectivity changes can be found in the right hemisphere or across the whole brain, except two, which exist in left hemisphere. These abnormal changes are visualized in Fig. 5 (abbreviations listed in Table 7). We also found that, during the AD conversion process, gradually increased connection strength appears in short distance correlations (e.g., PHG.L to PHG.R, PreCG.R to PCG.R, IPL.L to STG.L, etc.) and gradually decreased connection strength appears in long distance correlations (e.g., IOG.L to ITG.R, PoCG.R to MTG.L, PHG.R to CUN.L, etc.). In our study, the inter-group connectivity with Euclidean distance greater than 75 mm is considered to be the long distance connectivity [29].

DISCUSSION

The present study introduced a novel feature extraction method to establish an individual cortical thickness network. We adequately considered the effects from both vertex thickness and regional mean

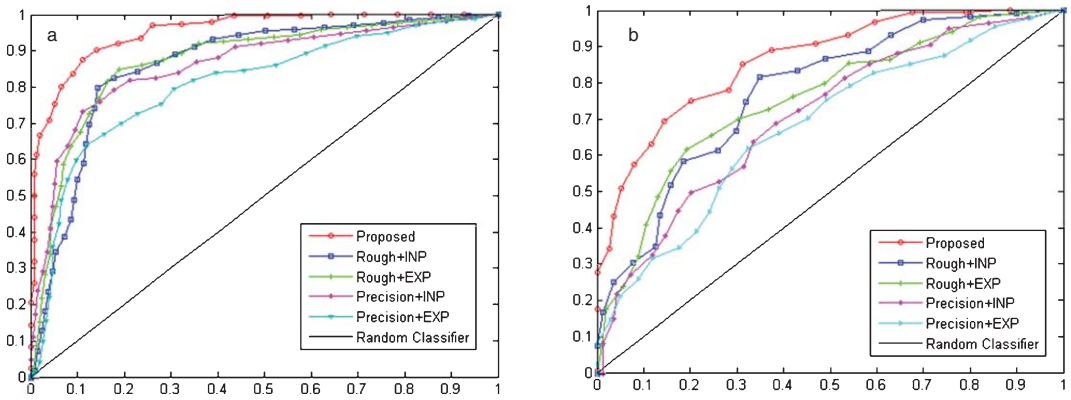

Fig. 4. ROC curve of different cases. (a) and (b) show the ROC curve of different combinations of distance and correlation calculation function in AD classification and prediction.

Table 6
Top 20 discriminative correlations in sMCI versus pMCI prediction

Proposed method					
Rank	Connectivity	p-value ($\times 10^{-5}$)	Rank	Connectivity	p-value ($\times 10^{-5}$)
1	Occipital – Temporal_Inf_R	0.0017	11	Parietal_Inf_L – Temporal_Sup_L	1.2823
2	**ParaHippocampal_L – ParaHippocampal_R**	**0.0039**	**12**	**Lingual_R – Temporal_Mid_R**	**1.3051**
3	Cuneus_L – SupraMarginal_R	0.2064	13	ParaHippocampal_R – Cuneus_L	1.7178
4	**ParaHippocampal_L – Lingual_L**	**0.3184**	**14**	**ParaHippocampal_R – Calcarine_L**	**1.7514**
5	Occipital_Sup_L – Temporal_Mid_R	0.5072	15	Occipital_Sup_R – Temporal_Mid_R	2.0996
6	**Postcentral_R – Temporal_Mid_L**	**0.8414**	**16**	**Paracentral_Lobule_R – Temporal_Inf_L**	**2.4837**
7	Occipital_Inf_L – Precuneus_R	0.8850	17	Postcentral_R – Angular_R	3.0974
8	**Precentral_R – Cingulum_Post_R**	**0.9964**	**18**	**Cuneus_L – Angular_R**	**3.3656**
9	Angular_L – Temporal_Pole_Sup_L	1.1151	19	Insula_L – ParaHippocampal_R	3.4965
10	**Temporal_Sup_L – Temporal_Sup_R**	**1.2767**	**20**	**Cuneus_L – Temporal_Mid_R**	**3.9507**

L, left; R, right. Bold letter means the correlations only occur in specific network.

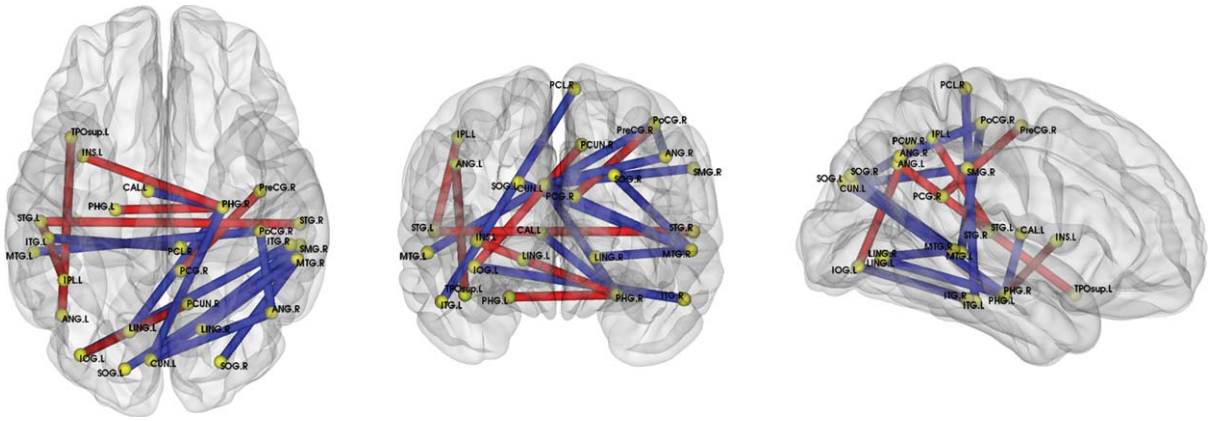

Fig. 5. Visualization of the top 20 discriminative correlations selected by t-test ($p < 0.05$, BH-FDR corrected). Red (blue) line means the average weight in sMCI group is larger (smaller) than it in pMCI group.

Table 7
Abbreviations of the Automated Anatomical Labeling (AAL) regions shown in Fig. 5

Region ID	AAL region	Abbreviation
1	Precentral	PreCG
2	Insula	INS
3	Cingulum_Post	PCG
4	ParaHippocampal	PHG
5	Calcarine	CAL
6	Cuneus	CUN
7	Lingual	LING
8	Occipital_Sup	SOG
9	Occipital_Inf	IOG
10	Postcentral	PoCG
11	Parietal_Inf	IPL
12	SupraMarginal	SMG
13	Angular	ANG
14	Precuneus	PCUN
15	Paracentral_Lobule	PCL
16	Temporal_Sup	STG
17	Temporal_Pole_Sup	TPOsup
18	Temporal_Mid	MTG
19	Temporal_Inf	ITG

cortical thickness when calculating the dissimilarity between brain regions. In other words, the local and global characteristics were combined to ensure accurate relationship measurement. The INP function, which could directly reflect the inverse variation between dissimilarity and connectivity, was applied to calculate the connectivity. Results suggest that our method outperformed previous studies in both cortical thickness and thickness correlations using large numbers of subjects from ADNI database.

Unlike morphological features or ROI-based features, which segment brain into regions and then explore each individual region independently without considering any inter-regional relations, correlative features are more complex, not limited to certain area, and rather include the abnormal alterations widely over the brain. We believe connectivity changes might contain discriminative characteristics and reveal the alterations between brain regions either adjacent or distant. In addition, as network could reflect the relationship between pairs of brain regions, which are

relatively less sensitive to the influence of individual diversities [41], we assume the correlation could be more robust than thickness. So far, since there is no well-recognized method for individual morphological network construction based on gray matter, we present a methodology of revealing internal relations in gray matter while retaining the diversity of single subject. Results show that correlative alterations are more discriminative than independent regional thickness (see Tables 2 and 3). It is noteworthy that the high specificity of 98.85% indicates our method has extremely low false diagnosis rate in AD; and the high AUC values (>0.91) in all the classification cases could reflect high precision and great power in automatic diagnosis. However, when combining such whole brain correlations with cortical thickness, performances are not as good as we expected. Improvements only can be observed in AD-NC separation and AD conversion prediction, with accuracies of 90.48% (AUC = 0.9607) and 78.38% (AUC = 0.8611), respectively, suggesting ROI-based features delivered some complementary information into correlations. Another interesting finding is that the accuracies drop a little when adding thickness into MCI classification, which is in contrast to the previous study [40], due to the fact that MCI is the middle stage between healthy control and dementia, which contains characteristics belonging to both sides. In addition, thickness of MCI in some areas could be very similar in some AD and NC individuals. Therefore, combining with thickness can promote the performance of classifying AD-like group (AD and pMCI) from NC-like group (NC and sMCI) to some extent, with the side effect that it may also bring redundancy or confused information into MCI classification. We also investigated the performance alteration when adding APOEε4 allele information and found huge improvements in AD classification (accuracy of 92.11%), which might due to the big gap between the proportions of APOEε4 allele carriers in pairs of groups.

We suggest that the individual network construction based on gray matter characteristics could be divided into two steps: dissimilarity measurement and correlation calculation. Dissimilarity measurement depends on the distance between two regions. In a word, if the distance is large, the dissimilarity would be large as well. Correlation calculation function is based on dissimilarity, where the correlation varies inversely as a function of dissimilarity. The explanation of why our network performed better might depend on following reasons: 1) Using combined distance. In our study, the combination of precision distance and rough distance was utilized to compute dissimilarity rather than using only regional mean cortical thickness. On one hand, we suggest that the rough distance could reflect the whole interrelation between two brain regions but ignore detailed changes, for instance, some vertex-based information are probably not taken into account. On the other hand, precision distance can probably reveal the regional changes in detail. For example, it can reflect the local variation if some parts of region A are thicker than region B, and vice versa. However, precision distance showed less discriminative power than rough distance, which might be caused by the average process taking too much non-differential distances into account. Indeed, we argue that precision distance still contains local alteration information, as the results were much higher than randomly classified. Finally, the combined distance was applied in order to take advantages from both sides. 2) Using INP function. As correlation is inversely proportional to dissimilarity, the INP was chosen as it can directly reflect this relationship rather than other functions. In fact, the connectivity calculation function is not limited to EXP and INP; other monotone bounded function, like cosine function (between 0 and π), could also be selected. Our aim is to test whether improvements exist when using different functions. Results suggest that correlation calculation function has an effect on the final classification performance, and INP-correlation surpasses the correlation derived from EXP in diagnosing MCI and AD. 3) Two-step feature selection method. The feature selection method in this article is a two-step procedure, combining both filter method and wrapper method, in order to take advantage from both sides. For example, it improved the accuracy with relative low computing complexity and can overcome overfitting problems. In our work, the two-step feature selection method mRMR + SVM-RFE was selected, due to three important factors: maximizing relevance, minimizing redundancy, and exploring complementarity.

The brain regions and correlations listed in Table 6 have been reported to have abnormal alterations in MCI and AD patients, as well as in AD conversion process, indicating our findings are consistent with previous publications, such as studies in following regions: parahippocampal gyri, lingual gyri and cingulum cortex [60–64], insula [65, 66], inferior temporal gyri and superior temporal gyri [63, 67, 68], cuneus, parietal lobule, precuneus cortex, postcentral gyri and cingulate cortex [33, 68–71], supramarginal gyri, angular gyri, temporal lobe, and occipital cortex [66, 68, 72]. In addition, the correlations mentioned above are located

either in the same hemisphere, or widely spread over the whole brain, suggesting the abnormalities caused by MCI and dementia have affected the entire brain rather than certain areas.

We also explored some connectivity changes in our network. Compared with AD patients, there were less correlation changes in the MCI group. Furthermore, the variation tendencies of most correlations in the MCI group are consistent with those in AD, which might suggest that MCI is the transition stage in the progression of AD. In Fig. 5, pMCI shows increased short distance inter-regional connectivity and decreased long distance inter-regional connectivity compared with the sMCI group, which is consistent with the findings of previous studies that the conversion process accompanies progressively increased short distance connectivity and progressively decreased long distance connectivity [29, 33]. These abnormal correlation changes could probably explain the existence of low global efficiency, high local efficiency [33, 73], and low efficiency of global information propagation [74] in the brain of patients with pMCI and AD.

While addressing some challenges, we have also identified a number of limitations in our proposed method. Firstly, the subjects we used in our work are only a portion of the ADNI database, which may not represent the pathological characteristics of large patient populations. Applying our methods to a larger sample size might reveal more convincing results. Secondly, as the brain atlas is an influential factor to classification accuracy [75, 76], more proper partitioning would probably lead to better results. Future work will combine more characteristics, for example, volume, area, and metabolic features, to establish a connectivity network that could describe abnormal changes in a more accurate way. In addition, optimal dissimilarity measurement and correlation calculation function also need to be discovered.

In summary, we proposed a novel approach of extracting a connectivity network pattern from an individual MRI. The correlation was calculated to represent the alteration between pairs of brain regions. We suggest that the correlation we proposed could better reflect the structural changes of MCI and AD. Excellent performance was achieved in both classification and prediction. Results show that correlative features, which reveal the alterations throughout the brain, greatly exceeded the performance of ROI-based features. When combined with cortical thickness, improvements can be observed in separating AD-like patients from normal controls. Furthermore, the dissimilarity measurement and correlation calculation function were proved to greatly affect the outcomes. In conclusion, morphological correlation could be a valuable characteristic for diagnosing AD and predicting its conversion. Our results also gave support to the feasibility of an individual morphological network.

ACKNOWLEDGMENTS

This work was supported by the National Key Basic Research and Development Program of China (973 program) Grant 2014CB744600, the National Natural Science Foundation of China Grant No. 61210010 and the National Key Basic Research and Development Program of China (973 program) Grant 2011CB711000.

Data collection and sharing for this project was funded by the Alzheimer's Disease Neuroimaging Initiative (ADNI) (National Institutes of Health Grant U01 AG024904) and DOD ADNI (Department of Defense award number W81XWH-12-2-0012). ADNI is funded by the National Institute on Aging, the National Institute of Biomedical Imaging and Bioengineering, and through generous contributions from the following: AbbVie, Alzheimer's Association; Alzheimer's Drug Discovery Foundation; Araclon Biotech; BioClinica, Inc.; Biogen; Bristol-Myers Squibb Company; CereSpir, Inc.; Eisai Inc.; Elan Pharmaceuticals, Inc.; Eli Lilly and Company; EuroImmun; F. Hoffmann-La Roche Ltd and its affiliated company Genentech, Inc.; Fujirebio; GE Healthcare; IXICO Ltd.; Janssen Alzheimer Immunotherapy Research & Development, LLC.; Johnson & Johnson Pharmaceutical Research & Development LLC.; Lumosity; Lundbeck; Merck & Co., Inc.; Meso Scale Diagnostics, LLC.; NeuroRx Research; Neurotrack Technologies; Novartis Pharmaceuticals Corporation; Pfizer Inc.; Piramal Imaging; Servier; Takeda Pharmaceutical Company; and Transition Therapeutics. The Canadian Institutes of Health Research is providing funds to support ADNI clinical sites in Canada. Private sector contributions are facilitated by the Foundation for the National Institutes of Health (http://www.fnih.org). The grantee organization is the Northern California Institute for Research and Education, and the study is coordinated by the Alzheimer's Disease Cooperative Study at the University of California, San Diego. ADNI data are disseminated by the Laboratory for Neuro Imaging at the University of Southern California.

Authors' disclosures available online (http://j-alz.com/manuscript-disclosures/15-0311r2).

REFERENCES

[1] Braa H, Braak E (1991) Neuropathological stageing of Alzheimer-related changes. *Acta Neuropathol* **82**, 239-259.

[2] Salzman C, Jeste D, Meyer RE, Cohen-Mansfield J, Cummings J, Grossberg G, Jarvik L, Kraemer H, Lebowitz B, Maslow K (2008) Elderly patients with dementia-related symptoms of severe agitation and aggression: Consensus statement on treatment options, clinical trials methodology, and policy. *J Clin Psychiatr* **69**, 889.

[3] Whall AL, Black ME, Groh CJ, Yankou DJ, Kupferschmid BJ, Foster NL (1997) The effect of natural environments upon agitation and aggression in late stage dementia patients. *Am J Alzheimers Dis Other Demen* **12**, 216-220.

[4] Flicker L (1999) Dementia reconsidered: The person comes first. *BMJ* **318**, 880.

[5] de la Torre JC (2004) Alzheimer's disease is a vasocognopathy: A new term to describe its nature. *Neurol Res* **26**, 517-524.

[6] Brookmeyer R, Gray S, Kawas C (1998) Projections of Alzheimer's disease in the United States and the public health impact of delaying disease onset. *Am J Public Health* **88**, 1337-1342.

[7] Smith MA, Harris PLR, Sayre LM, Beckman JS, Perry G (1997) Widespread peroxynitrite-mediated damage in Alzheimer's disease. *J Neurosci* **17**, 2653-2657.

[8] Reisberg B, Ferris SH, de Leon MJ, Crook T (1982) The Global Deterioration Scale for assessment of primary degenerative dementia. *Am J Psychiatr* **139**, 1136-1139.

[9] Brookmeyer R, Johnson E, Ziegler-Graham K, Arrighi HM (2007) Forecasting the global burden of Alzheimer's disease. *Alzheimers Dement* **3**, 186-191.

[10] Morris JC, Cummings J (2005) Mild cognitive impairment (MCI) represents early-stage Alzheimer's disease. *J Alzheimers Dis* **7**, 235-239.

[11] Petersen RC, Doody R, Kurz A, Mohs RC, Morris JC, Rabins PV, Ritchie K, Rossor M, Thal L, Winblad B (2001) Current concepts in mild cognitive impairment. *Arch Neurol* **58**, 1985-1992.

[12] Bischkopf J, Busse A, Angermeyer M (2002) Mild cognitive impairment1–A review of prevalence, incidence and outcome according to current approaches. *Acta Psychiatr Scand* **106**, 403-414.

[13] Grundman M, Petersen RC, Ferris SH, Thomas RG, Aisen PS, Bennett DA, Foster NL, Jack CR Jr, Galasko DR, Doody R (2004) Mild cognitive impairment can be distinguished from Alzheimer disease and normal aging for clinical trials. *Arch Neurol* **61**, 59-66.

[14] Galimberti D, Scarpini E (2012) Progress in Alzheimer's disease. *J Neurol* **259**, 201-211.

[15] Sidman RL, Rakic P (1973) Neuronal migration, with special reference to developing human brain: A review. *Brain Res* **62**, 1-35.

[16] Green C, Bavelier D (2008) Exercising your brain: A review of human brain plasticity and training-induced learning. *Psychol Aging* **23**, 692.

[17] Huttenlocher PR (1990) Morphometric study of human cerebral cortex development. *Neuropsychologia* **28**, 517-527.

[18] Mendez MF, Ghajarania M, Perryman KM (2002) Posterior cortical atrophy: Clinical characteristics and differences compared to Alzheimer's disease. *Dement Geriatr Cogn Disord* **14**, 33-40.

[19] Blessed G, Tomlinson BE, Roth M (1968) The association between quantitative measures of dementia and of senile change in the cerebral grey matter of elderly subjects. *Br J Psychiatry* **114**, 797-811.

[20] Lehtovirta M, Soininen H, Laakso MP, Partanen K, Helisalmi S, Mannermaa A, Ryynanen M, Kuikka J, Hartikainen P, Riekinnen PJ (1996) SPECT and MRI analysis in Alzheimer's disease: Relation to apolipoprotein E epsilon 4 allele. *J Neurol Neurosurg Psychiatry* **60**, 644-649.

[21] Verghese PB, Castellano JM, Holtzman DM (2011) Apolipoprotein E in Alzheimer's disease and other neurological disorders. *Lancet Neurol* **10**, 241-252.

[22] Drzezga A, Grimmer T, Riemenschneider M, Lautenschlager N, Siebner H, Alexopoulus P, Minoshima S, Schwaiger M, Kurz A (2005) Prediction of individual clinical outcome in MCI by means of genetic assessment and 18F-FDG PET. *J Nucl Med* **46**, 1625-1632.

[23] Willette AA, Calhoun VD, Egan JM, Kapogiannis D, Alzheimer's Disease Neuroimaging Initiative (2014) Prognostic classification of mild cognitive impairment and Alzheimer's disease: MRI independent component analysis. *Psychiatry Res* **224**, 81-88.

[24] Hall A, Muñoz-Ruiz M, Mattila J, Koikkalainen J, Tsolaki M, Mecocci P, Kloszewska I, Vellas B, Lovestone S, Visser PJ (2015) Generalizability of the disease state index prediction model for identifying patients progressing from mild cognitive impairment to Alzheimer's disease. *J Alzheimers Dis* **44**, 79-92.

[25] Wolz R, Aljabar P, Hajnal JV, Lötjönen J, Rueckert D, Alzheimer's Disease Neuroimaging Initiative (2012) Nonlinear dimensionality reduction combining MR imaging with non-imaging information. *Med Image Anal* **16**, 819-830.

[26] Park HJ, Friston K (2013) Structural and functional brain networks: From connections to cognition. *Science* **342**, 1238411.

[27] Li Y, Liu Y, Li J, Qin W, Li K, Yu C, Jiang T (2009) Brain anatomical network and intelligence. *PLoS Comp Biol* **5**, e1000395.

[28] Zalesky A, Fornito A, Bullmore ET (2010) Network-based statistic: Identifying differences in brain networks. *Neuroimage* **53**, 1197-1207.

[29] He Y, Chen ZJ, Evans AC (2007) Small-world anatomical networks in the human brain revealed by cortical thickness from MRI. *Cereb Cortex* **17**, 2407-2419.

[30] Brier MR, Thomas JB, Fagan AM, Hassenstab J, Holtzman DM, Benzinger TL, Morris JC, Ances BM (2014) Functional connectivity and graph theory in preclinical Alzheimer's disease. *Neurobiol Aging* **35**, 757-768.

[31] Dai Z, He Y (2014) Disrupted structural and functional brain connectomes in mild cognitive impairment and Alzheimer's disease. *Neurosci Bull* **30**, 217-232.

[32] Liu Z, Zhang Y, Yan H, Bai L, Dai R, Wei W, Zhong C, Xue T, Wang H, Feng Y, You Y, Zhang X, Tian J (2012) Altered topological patterns of brain networks in mild cognitive impairment and Alzheimer's disease: A resting-state fMRI study. *Psychiatry Res* **202**, 118-125.

[33] Yao Z, Zhang Y, Lin L, Zhou Y, Xu C, Jiang T (2010) Abnormal cortical networks in mild cognitive impairment and Alzheimer's disease. *PLoS Comp Biol* **6**, e1001006.

[34] Chen G, Ward BD, Xie C, Li W, Wu Z, Jones JL, Franczak M, Antuono P, Li S-J (2011) Classification of Alzheimer disease, mild cognitive impairment, and normal cognitive status with large-scale network analysis based on resting-state functional MR imaging. *Radiology* **259**, 213-221.

[35] Jie B, Zhang D, Gao W, Wang Q, Wee C, Shen D (2014) Integration of Network Topological and Connectivity Properties for Neuroimaging Classification. *IEEE Trans Biomed Eng* **61**, 576-588.

[36] Jie B, Zhang D, Wee CY, Shen D (2014) Topological graph kernel on multiple thresholded functional connectivity

networks for mild cognitive impairment classification. *Hum Brain Mapp* **35**, 2876-2897.

[37] Shao J, Myers N, Yang Q, Feng J, Plant C, Böhm C, Förstl H, Kurz A, Zimmer C, Meng C (2012) Prediction of Alzheimer's disease using individual structural connectivity networks. *Neurobiol Aging* **33**, 2756-2765.

[38] Wee CY, Yap PT, Li W, Denny K, Browndyke JN, Potter GG, Welsh-Bohmer KA, Wang L, Shen D (2011) Enriched white matter connectivity networks for accurate identification of MCI patients. *Neuroimage* **54**, 1812-1822.

[39] Raj A, Mueller SG, Young K, Laxer KD, Weiner M (2010) Network-level analysis of cortical thickness of the epileptic brain. *Neuroimage* **52**, 1302-1313.

[40] Wee CY, Yap PT, Shen D (2013) Prediction of Alzheimer's disease and mild cognitive impairment using cortical morphological patterns. *Hum Brain Mapp* **34**, 3411-3425.

[41] Dai D, He H, Vogelstein JT, Hou Z (2012) Accurate prediction of AD patients using cortical thickness networks. *Mach Vis Appl* **24**, 1445-1457.

[42] Tijms BM, Moller C, Vrenken H, Wink AM, de Haan W, van der Flier WM, Stam CJ, Scheltens P, Barkhof F (2013) Single-subject grey matter graphs in Alzheimer's disease. *PLoS One* **8**, e58921.

[43] Tijms BM, Series P, Willshaw DJ, Lawrie SM (2012) Similarity-based extraction of individual networks from gray matter MRI scans. *Cereb Cortex* **22**, 1530-1541.

[44] Folstein MF, Folstein SE, McHugh PR (1975) "Mini-mental state": A practical method for grading the cognitive state of patients for the clinician. *J Psychiatr Res* **12**, 189-198.

[45] Morris JC (1993) The Clinical Dementia Rating (CDR): Current version and scoring rules. *Neurology* **43**, 2412-2414.

[46] Sled JG, Zijdenbos AP, Evans AC (1998) A nonparametric method for automatic correction of intensity nonuniformity in MRI data. *IEEE Trans Med Imag* **17**, 87-97.

[47] Tong T, Wolz R, Gao Q, Guerrero R, Hajnal JV, Rueckert D (2014) Multiple instance learning for classification of dementia in brain MRI. *Med Image Anal* **18**, 808-818.

[48] Tzourio-Mazoyer N, Landeau B, Papathanassiou D, Crivello F, Etard O, Delcroix N, Mazoyer B, Joliot M (2002) Automated anatomical labeling of activations in SPM using a macroscopic anatomical parcellation of the MNI MRI single-subject brain. *Neuroimage* **15**, 273-289.

[49] Guyon I, Elisseeff A (2003) An introduction to variable and feature selection. *J Mach Learn Res* **3**, 1157-1182.

[50] Hoque N, Bhattacharyya DK, Kalita JK (2014) MIFS-ND: A mutual information-based feature selection method. *Expert Syst Appl* **41**, 6371-6385.

[51] Peng H, Long F, Ding C (2005) Feature selection based on mutual information criteria of max-dependency, max-relevance, and min-redundancy. *IEEE Trans Pattern Anal Mach Intell* **27**, 1226-1238.

[52] Guyon I, Weston J, Barnhill S, Vapnik V (2002) Gene selection for cancer classification using support vector machines. *Mach Learn* **46**, 389-422.

[53] Brown G, Pocock A, Zhao M-J, Luján M (2012) Conditional likelihood maximisation: A unifying framework for information theoretic feature selection. *J Mach Learn Res* **13**, 27-66.

[54] Vapnik V (2000) *The Nature of Statistical Learning Theory,* Springer.

[55] Chang C-C, Lin C-J (2011) LIBSVM: A library for support vector machines. *ACM Trans Intell Syst Technol* **2**, 27.

[56] Hertz T, Hillel AB, Weinshall D (2006) Learning a kernel function for classification with small training samples. *In ICML 2006: Proceedings of the 23rd International Conference on Machine Learning*, ACM, New York, pp. 401-408.

[57] Drzezga A, Grimmer T, Riemenschneider M, Lautenschlager N, Siebner H, Alexopoulus P, Minoshima S, Schwaiger M, Kurz A (2005) Prediction of individual clinical outcome in MCI by means of genetic assessment and (18)F-FDG PET. *J Nucl Med* **46**, 1625-1632.

[58] Benjamini Y, Hochberg Y (1995) Controlling the false discovery rate: A practical and powerful approach to multiple testing. *J R Stat Soc Series B Stat Methodol*, 289-300.

[59] Benjamini Y, Krieger AM, Yekutieli D (2006) Adaptive linear step-up procedures that control the false discovery rate. *Biometrika* **93**, 491-507.

[60] Yao Z, Hu B, Liang C, Zhao L, Jackson M (2012) A longitudinal study of atrophy in amnestic mild cognitive impairment and normal aging revealed by cortical thickness. *PLoS One* **7**, e48973.

[61] Chincarini A, Bosco P, Calvini P, Gemme G, Esposito M, Olivieri C, Rei L, Squarcia S, Rodriguez G, Bellotti R, Cerello P, De Mitri I, Retico A, Nobili F (2011) Local MRI analysis approach in the diagnosis of early and prodromal Alzheimer's disease. *Neuroimage* **58**, 469-480.

[62] Di Paola M, Macaluso E, Carlesimo G, Tomaiuolo F, Worsley K, Fadd L, Caltagirone C (2007) Episodic memory impairment in patients with Alzheimer's disease is correlated with entorhinal cortex atrophy. A voxel-based morphometry study. *J Neurol* **254**, 774-781.

[63] Liu Y, Paajanen T, Zhang Y, Westman E, Wahlund LO, Simmons A, Tunnard C, Sobow T, Mecocci P, Tsolaki M, Vellas B, Muehlboeck S, Evans A, Spenger C, Lovestone S, Soininen H, AddNeuroMed C (2011) Combination analysis of neuropsychological tests and structural MRI measures in differentiating AD, MCI and control groups–the AddNeuroMed study. *Neurobiol Aging* **32**, 1198-1206.

[64] Pihlajamäki M, Sperling RA (2008) fMRI: Use in early Alzheimer's disease and in clinical trials. *Future Med* **3**, 409-421.

[65] Misra C, Fan Y, Davatzikos C (2009) Baseline and longitudinal patterns of brain atrophy in MCI patients, and their use in prediction of short-term conversion to AD: Results from ADNI. *Neuroimage* **44**, 1415-1422.

[66] Chételat G, Desgranges B, Landeau B, Mézenge F, Poline J, De La Sayette V, Viade F, Eustache F, Baron J-C (2008) Direct voxel-based comparison between grey matter hypometabolism and atrophy in Alzheimer's disease. *Brain* **131**, 60-71.

[67] Han Y, Wang J, Zhao Z, Min B, Lu J, Li K, He Y, Jia J (2011) Frequency-dependent changes in the amplitude of low-frequency fluctuations in amnestic mild cognitive impairment: A resting-state fMRI study. *Neuroimage* **55**, 287-295.

[68] Risacher SL, Saykin AJ, West JD, Shen L, Firpi HA, McDonald BC (2009) Baseline MRI predictors of conversion from MCI to probable AD in the ADNI cohort. *Curr Alzheimer Res* **6**, 347.

[69] Davatzikos C, Bhatt P, Shaw LM, Batmanghelich KN, Trojanowski JQ (2011) Prediction of MCI to AD conversion. via MRI, CSF biomarkers, and pattern classification. *Neurobiol Aging* **32 2322**, e2319-e2327.

[70] Matsuda H, Kitayama N, Ohnishi T, Asada T, Nakano S, Sakamoto S, Imabayashi E, Katoh A (2002) Longitudinal evaluation of both morphologic and functional changes in the same individuals with Alzheimer's disease. *J Nucl Med* **43**, 304-311.

[71] Wang L, Goldstein FC, Veledar E, Levey AI, Lah JJ, Meltzer CC, Holder CA, Mao H (2009) Alterations in cortical thickness and white matter integrity in mild cognitive impairment

measured by whole-brain cortical thickness mapping and diffusion tensor imaging. *Am J Neuroradiol* **30**, 893-899.

[72] Wang PJ, Saykin AJ, Flashman LA, Wishart HA, Rabin LA, Santulli RB, McHugh TL, MacDonald JW, Mamourian AC (2006) Regionally specific atrophy of the corpus callosum in AD, MCI and cognitive complaints. *Neurobiol Aging* **27**, 1613-1617.

[73] He Y, Chen Z, Evans A (2008) Structural insights into aberrant topological patterns of large-scale cortical networks in Alzheimer's disease. *J Neurosci* **28**, 4756-4766.

[74] Achard S, Bullmore E (2007) Efficiency and cost of economical brain functional networks. *PLoS Comp Biol* **3**, e17.

[75] Min R, Wu G, Cheng J, Wang Q, Shen D (2014) Multi-atlas based representations for Alzheimer's disease diagnosis. *Hum Brain Mapp* **35**, 5052-5070.

[76] Ota K, Oishi N, Ito K, Fukuyama H, Group S-JS (2014) A comparison of three brain atlases for MCI prediction. *J Neurosci Methods* **221**, 139-150.